Eur Biophys J (2008) 37:1167–1174
DOI 10.1007/s00249-008-0294-z

ORIGINAL PAPER

Charge stabilization in reaction center protein investigated by optical heterodyne detected transient grating spectroscopy

Hiroko Ohmori · László Nagy · Márta Dorogi · Masahide Terazima

Received: 10 September 2007 / Revised: 14 February 2008 / Accepted: 26 February 2008 / Published online: 11 March 2008

Abstract Photosynthetic reaction center (RC) pigment protein complex converts the free energy of light into chemical potential of charge pairs with extremely high efficiency. A transient phase in the absorption spectrum in the sub-millisecond time scale is expected to be especially important to examine the conformational gating model of the $Q_A^-Q_B$ to $Q_AQ_B^-$ (here Q_A and Q_B are the primary and secondary quinone type electron acceptors, respectively) electron transport. Essential kinetic components at few tens of microseconds scale and at around 200 μs have been suggested. We investigated the conformation change of RCs using heterodyne detection of the laser-induced transient grating method. An about 25 μs dynamics was observed, which coincides with the one described by the conformational gating model and possibly related to the nonadiabatic intrinsic $Q_A^-Q_B$ to $Q_AQ_B^-$ electron transport. The relative intensity of this component decreased with increasing quinone concentration indicating an initial $(P^+Q_A^-)_1$ or a relaxed $(P^+Q_A^-)_2$ conformational substate. We did not find the decay component at few hundreds of microseconds time scale indicating that there is no large displacement in the RC structure if Q_B is present. The diffusion coefficient of the RC/LDAO detergent micelles calculated from the kinetic component was $D = 3.8 \times 10^{-11}$ m^2/s that agrees fairly well with the number estimated from the Einstein–Stokes relationship, and relates to a hydrodynamic diameter of 11.4 nm of the RC in LDAO micellar solution.

Keywords Transient grating · Heterodyne detection · Reaction centers

Regional Biophysics Conference of the National Biophysical Societies of Austria, Croatia, Hungary, Italy, Serbia, and Slovenia.

H. Ohmori · M. Terazima
Department of Chemistry, Graduate School of Science, Kyoto University, Kyoto 6068502, Japan

L. Nagy (✉) · M. Dorogi
Institute of Medical Physics and Biophysics, University of Szeged, Egyetem u. 2, 6722 Szeged, Hungary
e-mail: lnagy@sol.cc.u-szeged.hu

Introduction

Photosynthetic reaction center (RC) is a pigment protein complex, which converts the free energy of light into chemical potential of charge pairs with extremely high efficiency. The quantum yield of the primary charge separation is almost 100% (Wraight and Clayton 1974), which could not be reproduced by humans up to now. This very efficient charge separation is assured by specific structural and functional requirements. Although, there are several types of RCs in living beings (PS-I and PS-II of plants and cyanobacteria, RCs of purple and green bacteria; Allen and Williams 1998) possibly developed from the ancient monomer protein, the basic processes they all perform are the same. These include (a) electron excitation by light, (b) charge separation and stabilization, (c) rearrangement of the dielectric medium and hydrogen bond interactions (including protonation and deprotonation of specific amino acids), and (d) conformational movements within the protein [including transition of (sub)states between dark and light adapted forms, and relaxation processes, Fig. 1].

Large numbers of homologies between the different types of proteins assure the main functions; however, there are substantial differences between the different RC types. Since the pioneering works of Arata and Parson (1981) and Kleinfeld et al. (1984), we know that RCs are in different

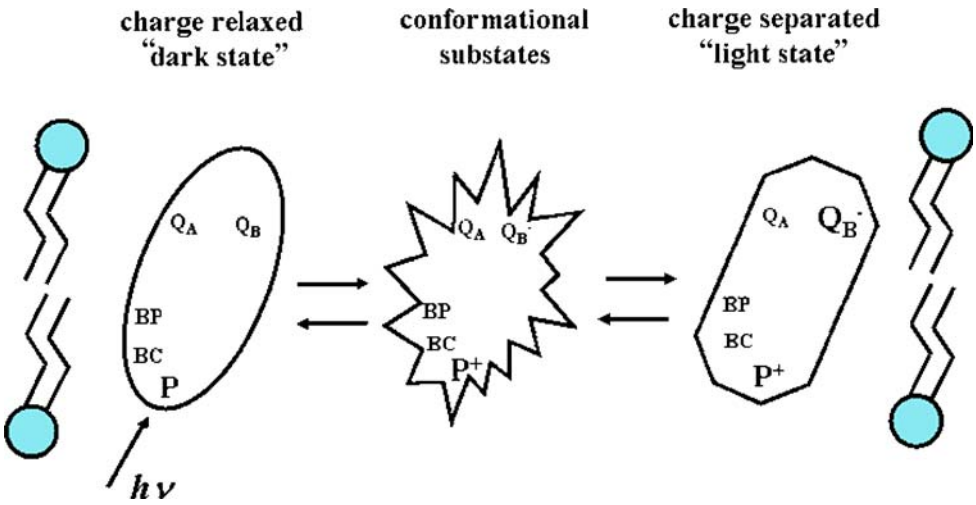

Fig. 1 Schematic representation of structural changes in reaction centers accompanying redox reactions. Here, *P* is the primary donor bacteriochlorophyll dimer, *BC* is the bacteriochlorophyll monomer, *BP* is the bacteriopheophityn, Q_A and Q_B are the quinone type primary and secondary quinone acceptors, respectively

conformational states during the charge relaxed dark to charge separated light transition. Kinetic and thermodynamic studies led to the conclusion that one of the electron transfer steps (namely the $Q_A^- Q_B \rightarrow Q_A Q_B^-$ reaction, here Q_A and Q_B are the primary and secondary quinone type electron acceptors, respectively) might be gated by conformational requirements (Graige et al. 1998). This theory seemed to be confirmed by resolving the structure of RCs adapted to dark and light conditions by atomic resolution (Stowell et al. 1997). This conformational gating process became one of the best studied processes in the last decade in many laboratories by using sophisticated, elegant methods including, for example, time resolved absorption spectroscopy (Tiede et al. 1996), photoacoustics (Mauzerall et al. 1995; Nagy et al. 2001), molecular simulations (Walden and Wheeler 2002; Alexov and Gunner 1999; Grafton and Wehler 1999), (time resolved) crystallographic studies (Baxter et al. 2004; Lancester 1998; McAulay et al. 2000; Pokkuluri et al. 2002; Fritzsch et al. 2002) and large numbers of FTIR spectroscopy (Remy and Klaus 2003; Breton 2004, 2007; Hermes et al. 2006).

Thanks to this huge effort of the researches, we have quite solid knowledge about the coupling of conformational changes to the electron transfer in the protein. It can be stated that (1) the quinone at the Q_B site can be situated in two distinct positions, the dark and light adapted states, that is, the distal and proximal positions, respectively (Stowell et al. 1997). (2) Only the proximal state is photochemically active (Graige et al. 1998). (3) The single reduced semiquinone, Q_B^-, is tightly bound to the proximal site. Nevertheless, different methods applied on different species resulted in substantial contradictory information. For example: (1) Although the distal–proximal transition seemed to be proved in *Rhodobacter sphaeroides*, the "Stowell structures" do not provide information about the kinetics of these structural movements. (2) Freeze-trapping crystallography found Q_B only in the proximal site in another species, *Rhodopseudomonas viridis* (Baxter et al. 2004). (3) No large-scale displacement in the Q_B site was found by time resolved FTIR experiments even in *R. sphaeroides* (Breton 2004; Remy and Klaus 2003). (4) By using site-specific mutagenesis, it seems that the position of the secondary quinone does not depend on the redox state of this molecule (Fritsch et al. 2002).

One reason for the contradictory information is that different methods were applied on different species under different conditions. The other reason can be that, although these methods are very sensitive, elegant, and accurate, none of them is suitable to give a detailed description of coupling kinetic, thermodynamic, and structural processes in a single experiment.

Here, we offer that optical heterodyne detection of the laser-induced transient grating signal (OHD-TG) fulfils these requirements appropriately. The time window of the observation is wide (from nanoseconds to seconds); the structural changes of the entire molecule (not only that of around the chromophore) can be measured; spectrally "silent" (no absorption change in the visible range) intermediates can also be detected; not only the equilibrium states, but also the transient intermediates, and irreversible reaction steps can be investigated. This method was successfully used for many applications including the kinetics and energetics of CO binding of myoglobine (Sakakura et al. 2001; Nishihara et al. 2004), the photocycle of the photoactive yellow protein (PYP, Kahn et al. 2006), determining diffusion coefficient of proteins and DNA (Baden and Terazima 2004), conformational changes of photosensor proteins (Inoue et al. 2004; Hazra et al. 2006; Eitoku et al. 2006; Nakasone et al. 2007).

The transient grating experiments are aimed to determine the structural changes accompanying electron transfer processes within the reaction center protein. The new

challenge of the research work would be to find the coupling between the kinetics and structural changes during the charge separation and stabilization and the subsequent electron and proton transfer accompanying conformation movements in the reaction center protein. In this work, we show that measuring OHD-TG signal is a unique and promising technique to solve this problem.

Principle

In the OHD-TG method, the TG signal intensity is enhanced by the interference between the signal field [$E_S(t)$] and a local oscillator (LO) field [E_{LO}] (Terazima 1999a, b; Rogers et al. 1997; Goodno et al. 1998). The principle has been described previously. Briefly, the detected light intensity under this heterodyne condition (I_{TG}) may be given by

$$I_{TG}(t) = \alpha|E_{LO} + E_S(t)|^2 = \alpha\left\{|E_{LO}|^2 + (E_{LO}E_S(t) + E_{LO}E_S(t)^*) + |E_S(t)|^2\right\} \quad (1)$$

where α is a constant. $|E_{LO}|^2$ gives a constant background of $I_{LO} = \alpha|E_{LO}|^2$. Under the present experimental conditions, $E_S(t)$ is very weak so that our observed time-dependent I_{TG} is given by only the cross term between E_{LO} and $E_S(t)$. $E_S(t)$ is proportional to the refractive index change $\delta n(t)$ under the present experimental conditions. Two main factors contribute to the refractive index change: the thermal effect [thermal grating, $\delta n_{th}(t)$] and a change in chemical species by the reaction [species grating, $\delta n_{spe}(t)$]. The species' grating component consists of the population and volume terms. Hence, we can monitor the temporal changes of the energy, absorption change, and molecular volume by using the OHD-TG signal.

When the energy relaxation is faster than the observation time range, the temporal profile of $\delta n_{th}(t)$ is determined by the thermal diffusion process, and is given by

$$\delta n_{th}(t) = \delta n_{th}^0 \exp\left(-D_{th}q^2 t\right) \quad (2)$$

The species grating signal intensity is given by the difference of the refractive index changes due to the reactant (δn_r) and product (δn_p). The time development of this component is determined by the reaction kinetics (absorption change and volume change). If the back reaction from the product to the reactant is comparable to the diffusion process;

$$R \xrightarrow{h\nu} P \xrightarrow{k} R$$

the temporal profile is given by

$$\delta n_{spe}(t) = \left\{\delta n_p^0 - \frac{k}{k + (D_r - D_p)q^2}\delta n_r^0\right\}\exp\left\{-\left(k + D_p q^2\right)t\right\} + \frac{\delta n_r^0 (D_r - D_p)q^2}{k + (D_r - D_p)q^2}\exp\left\{-D_r q^2 t\right\} \quad (3)$$

where D_r and D_p are diffusion coefficients of the reactant and the product, respectively. Furthermore, $\delta n_r(>0)$ and $\delta n_p(>0)$ are, respectively, the initial refractive index changes due to the presence of the reactant and the product.

Materials and methods

Sample preparations

R. sphaeroides R-26 cells were grown photoheterotrophically under anaerobic conditions. RCs were prepared by detergent (LDAO, N,N-dimethyldodecylamine-*N*-oxide) solubilization followed by ammonium sulphate precipitation and DEAE Sephacell anion exchange chromatography (Tandori et al. 1995). Both the primary (Q_A) and the secondary (Q_B) quinones were extracted out according to Okamura et al. (1975). RCs having different quantity of quinones were prepared by adding calculated amounts of ubiquinone-10 (UQ-10). The quinone/RC ratio was checked by kinetic absorption change measurement.

Transient grating measurements

An excitation laser beam (from the second harmonics of a Nd:YAG laser, $\lambda = 532$ nm, $\tau \sim 10$ ns) and a cw IR beam (YAG, 1,064 nm) were split by a transmission grating (optical mask) and the first order diffracted beams were combined again on the sample using a concave mirror. One of the cw IR beams was used for the probe beam of the TG signal. The other beam intensity was attenuated about 1/100 by a neutral density filter for the use of the local LO light. The filter was slightly tilted and used for a fine adjustment of the phase of the LO field to the probe field by changing the optical path length inside the filter. The LO light intensity was detected by a photo-diode. The LO light intensity could be varied not only by the interference between the signal and the LO light (the OHD-TG signal), but also by other contributions, such as the transient lens signal created by the pump beam (Terazima 1998). The OHD-TG signal was obtained by subtracting the LO light intensity without the probe beam from that with the probe beam.

The spacing of the grating fringe, equivalently, the grating wavenumber, was measured by the decay rate constant of the thermal grating signal from a calorimetric standard sample [bromocresol purple (BCP)]. The signal

was averaged and stored by a digital oscilloscope (Tektronics, TDS-520, Nishihara et al. 2004). For checking the sample conditions, the probe beam was blocked and the thermal lens component was measured. In some experiments, absorption change was monitored by a He–Ne laser (590 nm) after the flash excitation. The block diagram of the experimental set up is seen in Fig. 2.

Results and discussion

In order to examine the sample conditions, we routinely measured the temporal profile of the LO light intensity without the probe beam. Since this signal mostly originated from the transient lens component, the temporal profile represented the reaction dynamics of the RC. In particular, the decay of the signal reflected the relaxation kinetics of the redox components i.e., $P^+Q_A^-$ and $P^+Q_AQ_B^-$ charge pairs, which are fairly well known in the literature from kinetic absorption measurements. In our samples, the signal decays with about 100 ms for the Q_A and 1 s for the Q_B sample (Fig. 3). Independently, we also measured the lifetime of the redox components by the flash photolysis method using another cw probe laser at 590 nm. The lifetime from the laser induced absorption signal agreed quite well with those from the transient lens signal, which confirmed that the transient lens signal represented the refractive index change due to the absorption change (population lens).

The OHD-TG signal was obtained by subtracting the LO intensity without the probe beam from that with the probe beam. Figure 4 shows the OHD-TG signals measured by using Q_A (no quinone at the Q_B site) and Q_B (the Q_B site is reconstituted by UQ-10) samples. The temporal profiles of both signals were reproduced well by a bi-exponential function. The determined rate constants are listed in Table 1.

The time constant of the initial decaying components of the signals was around 25 μs (Table 1). Under the same conditions, the decay time constant of the thermal grating signal from the calorimetric reference sample was 15 μs, which was different from this value. Furthermore, the thermal grating signal from the calorimetric reference sample with the same absorbance as that of the RC sample was negligibly weak under the same conditions. Therefore, the decay component observed for the RC sample was not the thermal grating signal, but it represented reaction dynamics of RC.

The time constants of the later decay component depended on the q^2-value. This q^2-dependence indicates that protein diffusion process contributed to this decay rate. In general, the decay of the OHD-TG signal is expressed by a bi-exponential function as described in the principle

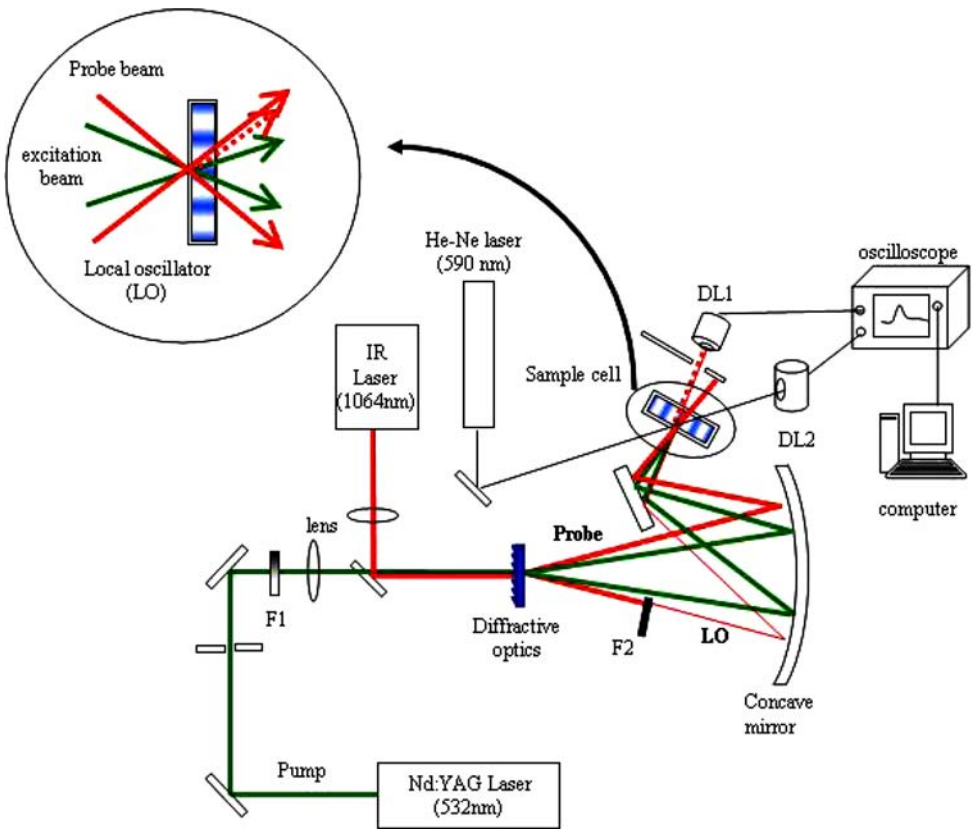

Fig. 2 The block diagram of the setup for measuring OHD-TG signal. The main parts are as follows: *F1* optical filter for changing the intensity of the actinic laser beam, *F2* optical filter for adjusting the phase of the measuring beam, *DL1* photodiode for detecting TG signal, *DL2* photodiode for detecting transient absorption signal

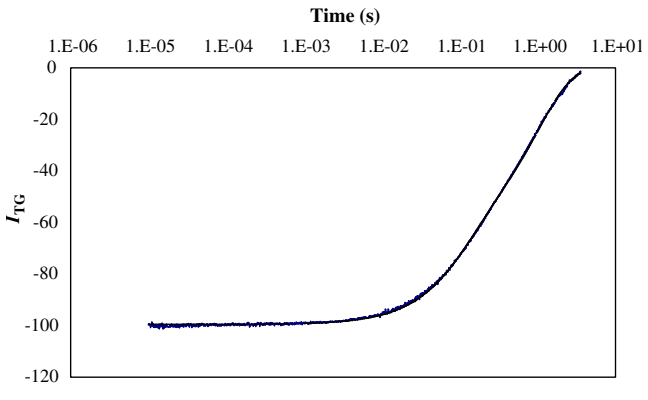

Fig. 3 The population lens component of the light-induced TG signal of photosynthetic reaction centers isolated from *R. sphaeroides* R-26. Measurement was done by the experimental setup outlined in Fig. 2 by blocking the probe light beam. *Solid black line* indicates the best fit of curve by the fitting parameters of $\tau_1 = 1.028$ s and $\tau_2 = 0.108$ s. The amplitudes of these components varied with the sample conditions (i.e., the yield of reconstitution of the Q_B site). RCs were suspended in 10 mM Tris, pH 8.0, 0.01% LDAO, 100 mM NaCl. The optical density of the sample was 1 at the excitation wavelength of 532 nm

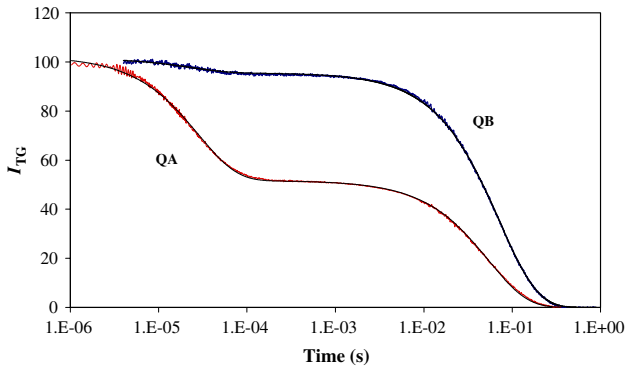

Fig. 4 The TG signal of one quinone/RC (Q_A) and two quinones/RC (Q_B, containing both the primary and the secondary quinones) samples as a function of time. The measuring conditions are same as described in Fig. 3, except that the probe beam was applied again to obtain the OHD-TG signal. *Solid black line* indicates the best fit of curves according to the data summarized in Table 1

section (Eq. 3). However, the later decay part of the signal was fitted well by a single exponential function. This fact indicates that D_p is almost the same as D_r so that the second term of Eq. 3 is very small. The negligible change in the diffusion coefficient by the photoreaction of RC is a striking contrast to the cases of photosensor proteins such as PYP, phototropins, YcgF (Inoue et al. 2004; Hazra et al. 2006; Eitoku et al. 2006; Nakasone et al. 2007). In these cases, D of photoproducts was generally smaller than that of the reactants. The reduction of D has been explained by conformation changes and/or dimerization/dissociation reactions of these sensor proteins. The very similar D_p to

Table 1 Summary of kinetic parameters of the thermal grating signal measured on isolated RCs containing only the primary (Q_A) and fully reconstituted secondary (Q_B) quinone acceptor site, presented in Fig. 4

	A_1 (%)	k_1 (s^{-1})	A_2 (%)	k_2 (s^{-1})
Q_A	50.0	18.4[a]	50.0	3.5×10^4
		(9.20)[b]		(2.8×10^{-5})
Q_B	94.1	13.9[a]	5.9	4.3×10^4
		(0.97)[b]		(2.3×10^{-5})

A (%) and k (s^{-1}) represent the amplitude and rate constant of the kinetic components, respectively. The rate constants of the corresponding ($P^+Q^- \rightarrow PQ$) chemical reactions are also indicated in brackets

[a] $k_1 = k_{obs}$: observed rate constant of the transient grating signal

[b] $k_1 = k_s$: rate constant of the chemical reaction ($P^+Q^- \rightarrow PQ$ charge recombination), calculated by using $k_{obs} = Dq^2 + k_s$

D_r of RC indicates that a conformation change of RC is rather minor, and a change in the hydrogen bonding network is not significant to change the RC/solvent environment interaction (i.e., friction for the translational diffusion).

Under a condition of $D_p \sim D_r$, the decay rate constant of the OHD-TG signal is given by $D_r q^2 + k$, where k is the rate constant of the charge recombination. Indeed, we found that the decay rate constant was proportional to q^2 and intercept at $q^2 = 0$ was about 100 ms for the Q_A and about 1 s for the Q_B sample, which agreed well with the observed rate constant from the population lens or transient absorption signal. From the slope of the plot, we determined the diffusion coefficient $D = 3.8 \times 10^{-11}$ m^2/s. The hydrodynamic diameter of the RC/LDAO micelles calculated from this value was 11.4 nm, which agrees fairly well with the particle size estimated from the crystal structure or AFM experiments (Dorogi et al. 2006).

Table 1 shows the decay parameters and related kinetic parameters for the Q_A and the fully reconstituted Q_B sample. The transient phase in the sub-millisecond time scale expected to be especially important because the conformational gating of the $Q_A^- Q_B$ to $Q_A Q_B^-$ electron transport suggests essential kinetic components at few tens of μs scale and at around 200 μs. To our surprise, we did not find decay component at few hundreds of microseconds time scale. The absence of this component implies that there is no such conformation change with this time constant or the volume change due to this change is very small (<ca. 1 cm^3/mol, cf. the molar volume of water is 18 cm^3/mol). However, interestingly, we did observe an about 25 μs (4×10^4 s^{-1}) dynamics for each samples and the relative intensity of this component is largest for the Q_A sample and decreased with increasing the concentration of quinone. When we added quinone, so that we got fully

reconstituted Q_B sample, this 25 μs component became very weak (ca. 5%). We propose that in the absence of secondary quinone, the $P^+Q_A^-$ charge separated state can be in the initial $(P^+Q_A^-\ldots)_1$ or in the relaxed conformation substate $(P^+Q_A^-\ldots)_2$, where (…) indicates the empty Q_B site.

In the presence of Q_B, the formation of the $(P^+Q_A^-\ldots)_2$ population is not favored. Because (...) is occupied by Q_B, the Q_A^- to Q_B electron transport occurs if the secondary quinone is in the active proximal position, so that the 25 μs dynamics become weaker with increasing quinone concentration. This does not accompany with larger conformational TG signal indicating possibly a less flexible protein structure if the Q_B site is occupied. Similarly, larger molecular volume change and entropy contribution to the free energy was measured for RC if the Q_A site was reconstituted (ΔV: 14.4 cm^3/mol, TΔS: 26%) compared to the RCs with fully reconstituted Q_B site (ΔV: 7.4 cm^3/mol, TΔS: 4%) by photoacoustic technique (Nagy et al. 2001). It must be noted that these later values are not related to the same process than the 25 μs dynamics exactly, because these appear very quickly after the excitation. They most probably related to the $P^+Q_A^-$ charge pair formation, at least within the lifetime of the laser pulse (few tens of ns; Nagy et al. 2001; Mauzerall et al. 1995; Edens et al. 2000).

Although transient absorption spectroscopy clearly shows electrochromic shift of the bacteriopheophytin absorption in the near infrared, possibly due to the reorganization of charges (Nagy et al. 2004; Tiede et al. 1996), this effect cannot be so large, or it can induce consecutive, compensating structural movements so that no overall volume change can be observed at few hundreds of microseconds. The structural rearrangement does not necessarily mean overall volume change along the reaction coordinate.

It must be noted that the lifetime we measured for the fast decaying component, 25 μs, is in the range of the lifetime of reaction paths to triplet formation [$^3(P^+I^-)$ and ^3P, for reference see Shuvalov and Parson 1981; Volk et al. 1995; Arellano et al. 2007] so that parallel mechanisms to charge pair formation or to charge recombination processes should not be ruled out. However, it does not look very reasonable that the low concentration of the triplet states, which are probably formed (Angerhofer et al. 1998; Marchanka et al. 2007; Turzó et al. 2000), contribute considerably to the transient grating signal. Note that the quantum yield of the competing prompt and delayed fluorescence of the primary donor in isolated bacterial reaction centers is about 10^{-4} and 10^{-9}, respectively (Zankel et al. 1968; Arata and Parson 1981; Woodbury et al. 1985; Turzó et al. 2000). Furthermore, the triplet lifetime under the air saturation condition should be shorter than microseconds due to the oxygen quenching and it cannot be 25 μs. Therefore, the observed dynamics cannot be due to the triplet state formation. Nevertheless, although the probability of triplet formation in our conditions is small (no secondary donor is present, primary qionone is oxidized, low probability for double excitation, oxygen is present), the discussion of the contribution of the triplet states to the transient grating would be important, but it needs more careful investigations and cannot be the scope of this conference paper.

Summary

In summary, we can state that optical heterodyne detection of the laser-induced transient grating signal is a very sensitive way to show kinetic components in photoreactions of photosynthetic reaction centers. Our results confirm that there is a kinetic component in the $Q_A^-Q_B$ to $Q_AQ_B^-$ electron transport at around 25 μs, which coincides with the one already described by the conformational gating model. Transient absorption change measurements indicate that there should be definite charge movements in this time scale (Tiede et al. 1996; Li et al. 1998; Nagy et al. 2004), which is possibly a consequence of the nonadiabatic intrinsic $Q_A^-Q_B$ to $Q_AQ_B^-$ electron transport (Cherepanov et al. 2001). Our results indicate that a structural rearrangement [possibly change in protonation states of specific amino acids (Li et al. 1998; Cherepanov et al. 2001; Breton 2007)] accompanies this charge movement only if the Q_B site is occupied. If the Q_B site is not occupied by quinone, the $P^+Q_A^-$ charge separated state can be in the initial $(P^+Q_A^-\ldots)_1$ or in the relaxed conformation substate $(P^+Q_A^-\ldots)_2$. Further investigations of the specific conditions of these components are in progress.

Acknowledgments This work was supported by the grant of Japan Society for Promotion of Science and also by the Grant-in-Aid (nos. 13853002 and 15076204 to M.T.) from the Ministry of Education, Science, Sports, and Culture in Japan.

References

Alexov EG, Gunner MR (1999) Calculated protein and proton motions coupled to electron transfer: electron transfer from Q_A^- to Q_B in bacterial photosynthetic reaction centers. Biochemistry 38:8253–8270

Allen JP, Williams JC (1998) Photosynthetic reaction centers. FEBS Lett 438:5–9

Angerhofer A, Bornhäuser F, Aust V, Hartwich G, Scheer H (1998) Triplet energy transfer in bacterial photosynthetic reaction centres. Biochim Biophys Acta 1365:404–420

Arata H, Parson WW (1981) Enthalpy and volume changes accompanying electron transfer from P-870 to quinones in *Rps. sphaeroides* reaction centers. Biochim Biophys Acta 636:70–81

Arellano JB, Yousef YA, Melo TB, Mohamad SBB, Cogdell RJ, Naqvi KR (2007) Formation and geminate quenching of singlet

oxygen in purple bacterial reaction center. J Photochem Photobiol B Biol 87:105–112

Baden N, Terazima M (2004) A novel method for measurement of diffusion coefficients of proteins and DNA in solution. Chem Phys Lett 393:539–545

Baxter RHG, Ponomarenko N, Sÿrajer V, Pahl R, Moffat K, Norris JR (2004) Time-resolved crystallographic studies of light-induced structural changes in the photosynthetic reaction center. Proc Natl Acad Sci USA 101:5982–5987

Breton J (2004) Absence of large-scale displacement of quinone Q_B in bacterial photosynthetic reaction centers. Biochemistry 43:3318–3326

Breton J (2007) Steady state FTIR spectra of the photoreduction of Q_A and Q_B in *Rhodobacter sphaeroides* reaction centers provide evidence against the presence of a proposed transient electron acceptor X between the two quinines. Biochemistry 46:4459–4465

Cherepanov DA, Krishtalik LI, Mulkidjanian AY (2001) Photosynthetic electron transfer controlled by the protein relaxation: analysis by Langevin stochastic approach. Biophys J 80:1033–1049

Dorogi M, Bálint Z, Mikó C, Vileno B, Milas M, Hernádi K, Forró L, Váró Gy, Nagy L (2006) Stabilization effect of single-walled carbon nanotubes on the functioning of photosynthetic reaction centers. J Phys Chem B 110:21473–21479

Edens GJ, Gunner MR, Xu Q, Mauzerall DC (2000) The enthalpy and entropy of reaction for formation of $P^+Q_A^-$ from excited reaction centers of *Rhodobacter sphaeroides*. J Am Chem Soc 122:1479–1485

Eitoku T, Zarate X, Kozhukh GV, Kim JI, Song PS, Terazima M (2006) Time-resolved detection of conformational changes in oat phytochrome A: time-dependent diffusion. Biophys J 91:3797–3804

Fritzsch G, Koepke J, Diem R, Kuglstatter A, Baciou L (2002) Charge separation induces conformational changes in the photosynthetic reaction centre of purple bacteria. Acta Crystallogr D Biol Crystallogr 58:1660–1663

Goodno GD, Dadusc G, Miller RJD (1998) Ultrafast heterodyne-detected transient-grating spectroscopy using diffractive optics. J Opt Soc Am B 15:1791–1794

Grafton AK, Wheeler RA (1999) Amino acid protonation states determine binding sites of the secondary ubiquinone and its anion in the *Rhodobacter sphaeroides* photosynthetic reaction center. J Phys Chem B 103:5380–5387

Graige MS, Feher G, Okamura MY (1998) Conformational gating of the electron transfer reaction $Q_A^-Q_B$–$Q_AQ_B^-$ in bacterial reaction centers of *Rhodobacter sphaeroides* determined by driving force assay. Proc Natl Acad Sci USA 95:11679–11684

Hazra P, Inoue K, Laan W, Hellingwerf KJ, Terazima M (2006) Tetramer formation kinetics in the signaling state of AppA monitored by time-resolved diffusion. Biophys J 91:654–661

Hermes S, Stachnik JM, Onidas D, Remy A, Hofman E, Gerwert K (2006) Proton uptake in the reaction center mutant L210DN from *Rhodobacter sphaeroides* via protonated water molecules. Biochemistry 45:13741–13749

Inoue K, Sasaki J, Morisaki M, Tokunaga F, Terazima M (2004) Time-resolved detection of the sensory rhodopsin II–transducer interaction. Biophys J 87:2587–2597

Khan JS, Imamoto Y, Kataoka M, Tokunaga F, Terazima M (2006) Time-resolved thermodynamics: heat capacity change of transient species during photo-reaction of PYP. J Am Chem Soc 128:1002–1008

Kleinfeld D, Feher G, Okamura MY (1984) Electron-transfer kinetics in photosynthetic reaction centers cooled to cryogenic temperatures in the charged separated state: evidence for light-induced structural changes. Biochemistry 23:5780–5786

Lancaster CRD (1998) Ubiquinone reduction and protonation in photosynthetic reaction centres from *Rhodopseudomonas viridis*: X-ray structures and their functional implications. Biochim Biophys Acta 1365:143–150

Li J, Gilroy D, Tiede DM, Gunner MR (1998) Kinetic phases in the electron transfer from $P^+Q_A^-Q_B$ to $P^+Q_AQ_B^-$ and the associated processes in *Rhodobacter sphaeroides* R-26 reaction centers. Biochemistry 37:2818–2829

Marchanka A, Paddock M, Lubitz W, Gastel M (2007) Low-temperature pulsed EPR study at 34 GHz of the triplet states of the primary electron donor P_{865} and the carotenoid in native and mutant bacterial reaction centers of *Rhodobacter sphaeroides*. Biochemistry 46(51):14782–14794

Mauzerall DC, Gunner MR, Zhang JW (1995) Volume contraction on photoexcitation of the reaction center from *Rhodobacter sphaeroides* R-26: internal probe of dielectrics. Biophys J 68:275–280

McAuley KE, Fyfe PK, Ridge JP, Cogdell RJ, Isaacs NW, Jones MR (2000) Ubiquinone binding, ubiquinone exclusion, and detailed cofactor conformation in a mutant bacterial reaction center. Biochemistry 39:15032–15043

Nagy L, Kiss V, Brumfeld V, Malkin S (2001) Thermal and structural changes of photosynthetic reaction centers characterized by photoacoustic detection with a broad frequency band hydrophone. Photochem Photobiol 74:81–87

Nagy L, Milano F, Dorogi M, Trotta M, Laczkó G, Szebényi K, Váró Gy, Agostiano A, Maróti P (2004) Protein/lipid interaction in bacterial photosynthetic reaction center: the role of phosphatidylcholine and phosphatidylglycerol in charge stabilization. Biochemistry 43:12913–12923

Nakasone Y, Ono T, Ishii A, Masuda S, Terazima M, (2007) Transient dimerization and conformational change of a BLUF protein: YcgF. J Am Chem Soc 129:7028–7035

Nishihara Y, Sakakura M, Kimura Y, Terazima M (2004) The escape process of carbon monoxide from myoglobin to solution at physiological temperature. J Am Chem Soc 126:11877–11888

Okamura MY, Isaacson RA, Feher G (1975) Primary acceptor in bacterial photosynthesis: obligatory role of ubiquinone in photoactive reaction centers of *Rhodopseudomonas sphaeroides*. Proc Natl Acad Sci USA 72:3491–3495

Pokkuluri PR, Laible PD, Deng YL, Wong TN, Hanson DK, Schiffer M (2002) The structure of a mutant photosynthetic reaction center shows unexpected changes in main chain orientations and quinone position. Biochemistry 41:5998–6007

Remy A, Klaus G (2003) Coupling of light-induced electron transfer to proton uptake in photosynthesis. Nat Struct Biol 10:637–644

Rogers JA, Fuchs M, Banet MJ, Hanselman JB, Logan R, Nelson KA (1997) Optical system for rapid materials characterization with the transient grating technique: application to nondestructive evaluation of thin films used in microelectronics. Appl Phys Lett 71:225–227

Sakakura M, Yamaguchi SY, Hirota N, Terazima M (2001) Dynamics of structure and energy of horse carboxymyoglobin after photodissociation of the carbon monoxide. J Am Chem Soc 123:4286–4294

Shuvalov VA, Parson WW (1981) Triplet-states of monomeric bacteriochlorophyll in vitro and of bacteriochlorophyll dimers in antenna and reaction center complexes. Biochim Biophys Acta 638:50–59

Stowell MHB, McPhillips TM, Rees DC, Soltis SM, Abresh E, Feher G (1997) Light induced structural changes in photosynthetic reaction center: implications for mechanism of electron-proton transfer. Science 276:812–816

Tandori J, Nagy L, Puskás A, Droppa M, Horváth G, Maróti P (1995) The Ile^{L229} –> Met mutation impairs the quinone binding to the

Q_B^-pocket in reaction centers of *Rhodobacter sphaeroides*. Photosynth Res 45:135–146

Terazima M (1998) Transient lens spectroscopy in a fast time scale. Isr J Chem 38:143–157

Terazima M (1999a) Optical heterodyne detected transient grating for studies of photochemical reactions and solution dynamics. Chem Phys Lett 304:343–349

Terazima M (1999b) Optical heterodyne detected transient grating for the separation of phase and amplitude gratings. J Phys Chem A 103:7401–7407

Tiede DM, Vazquez J, Cordova J, Marone PA (1996) Time resolved electrochromism associated with the formation of quinone anions in the *Rhodobacter sphaeroides* R26 reaction center. Biochemistry 35:10763–10775

Turzó K, Laczkó G, Filus Z, Maróti P (2000) Quinone-dependent delayed fluorescence from the reaction center of photosynthetic bacteria. Biophys J 79:14–25

Volk M, Ogrodnik A, Michel-Beyerle M-E (1995) The recombination dynamics of the radical pair P+H− in external magnetic and electric fields. In: Blankensip RE Madigan MT, Bauer CE (eds) Anoxygenic photosynthetic bacteria. Kluwer, Dordrecht, pp 595–626

Walden SE, Wheeler RA (2002) Protein conformational gate controlling binding site preference and migration for ubiquinone-B in the photosynthetic reaction center of *Rhodobacter sphaeroides*. J Phys Chem B 106:3001–3006

Woodbury NW, Becker M, Middendorf D, Parson WW (1985) Pikosecond kinetics of the initial photochemical electron transfer reaction in bacterial photosynthetic reaction centers. Biochemistry 24:7516–7521

Wraight CA, Clayton R (1974) The absolute quantum efficiency of bacteriochlorophyll photooxidation in reaction centres of *Rhodopseudomonas sphaeroides*. Biochim Biophys Acta 333:246–260

Zankel KL, Reed DW, Clayton RK (1968) Fluorescence and photochemical quenching in photosynthetic reaction centers. Proc Natl Acad Sci USA 61:1243–1249